Online Supplemental Material for

Anishkin et al. **http://www.jgp.org/cgi/doi/10.1085/jgp.200409118**

200409118 Supplemental Material

SECTION 1

Although the linear free energy (LEFR) analysis for a multistate mechanosensitive channel has been used previously (Sukharev et al., 1999), here we present a brief basic description. A generic multiwell profile for the transition is presented in Fig. S1. The reaction proceeds through several states represented as a series of wells along the in-plane area axis (ΔA), which represents the reaction coordinate for an expanding channel gated by lateral tension (γ). The tension distorts the free energy profile $E(\Delta A)$ by adding the linear term $-\gamma\Delta$A, making wider conformations more favorable. The ratio of occupancies of any two wells (not necessarily adjacent) at equilibrium obeys the Boltzmann distribution:

$$P_j/P_i = \exp[-(\Delta E_{ji} - \gamma\Delta A_{ji})/kT].$$

The slope of $\ln(P_j/P_i)$ on tension would be equal to $\Delta A_{ji}/kT$, thus reporting on the area difference between the two states (on the graph these would be positions of the bottoms of the wells). For two adjacent states separated by a single barrier, the two rate constants can be written in the Eyring's form:

$$k_{ij} = k_0\exp[-(\Delta h_b - \gamma\Delta A_{bi})/kT]$$

and

$$k_{ji} = k_0\exp[-(\Delta h_b - \Delta E_{ji} + \gamma\Delta A_{jb})/kT],$$

where Δh_b is the height of the barrier looking from the left well, $\Delta h_b - \Delta E_{ji}$ is the height of the barrier as seen from the right well, and ΔA_{bi} and ΔA_{jb} are the area differences between the bottoms of each well to the tip of the barrier. By taking logarithms and then derivatives on γ, one may see that the logarithmic slopes of the rate constants directly report on the differences between the equilibrium positions of the states and of the rate-limiting barrier.

$$\frac{d\ln k_{ij}}{d\gamma} = \Delta A_{bi}/kT$$

and

$$\frac{d\ln k_{ji}}{d\gamma} = -\Delta A_{jb}/kT$$

If two discernable states are separated with a series of unequal barriers with one dominating, this simple formalism may assign the approximate position of the dominating barrier. Note that in this representation, we do not consider the absolute height of the barrier as it would depend on the arbitrarily frequency factor k_o (Andersen, 1999). Because k_o is excluded from the last two equations, the position of the barrier on the reaction coordinate (ΔA) is independent of the frequency factor.

SECTION 2

Energy Estimations

To relate and properly separate energy profiles for transitions in different mutants, we took into account the solvation and electrostatic effects of gain-of-function mutations. To assess statistically the conformations of side chains of residues 22 and 23 subjected to substitutions, short MD simulations of modeled open conformation were performed using the NAMD program (Kale et al., 1999). The molecular model of the open state that satisfies the 3.2-nS unitary conductance (conformation 11) was taken from Sukharev et al. (2001b). The model with restrained backbone was heated in vacuo to 310 K for 10 ps to introduce slight thermal disorder in the sidechain packing. The hydration energy per atom was calculated using the GETAREA web-based software (Fraczkiewicz and Braun, 2002) with the probe radius of 1.4 Å and atomic solvation parameters taken from Wesson and Eisenberg (1992). The hy-

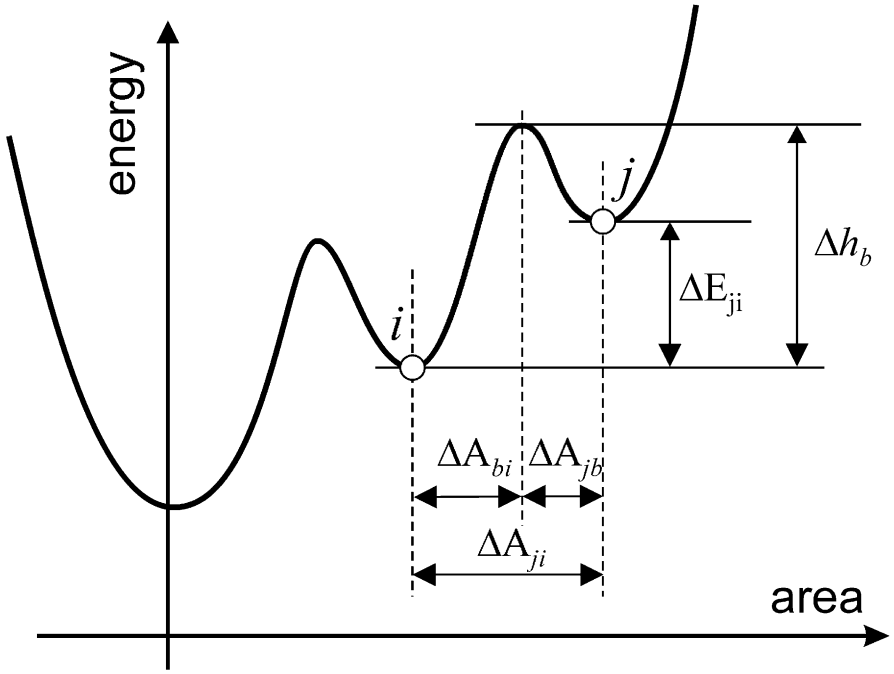

FIGURE S1. Free energy profile for a generic sequential transition over several states. The energy and space parameters for two adjacent wells and the barrier are denoted. See SECTION 1.

dration energy difference introduced by a particular mutation was estimated as the difference of hydration energy of the native residue (V23 or G22) and that of the substitute (T or D for V23, or N for G22) in similar positions in an α helix.

A rough estimation of the electrostatic repulsion between the five negatively charged aspartates introduced in V23D mutant (assuming all five acidic residues are dissociated) was performed for the model of the open state of MscL. The system was represented as five point charges positioned on the vertices of a pentagon with the side of 20 Å with dielectric permeability of 80 in the pentagon and of six outside it, imitating water-filled MscL pore with hydrophobic lining in the horizontal protein slice containing V23.

REFERENCES

Andersen, O.S. 1999. Graphic representation of the results of kinetic analysis. *J. Gen. Physiol.* 114:589–590.

Sukharev, S.I., W.J. Sigurdson, C. Kung, and F. Sachs. 1999. Energetic and spatial parameters for gating of the bacterial large conductance mechanosensitive channel, MscL. *J. Gen. Physiol.* 113:525–540.

Sukharev, S., S.R. Durell, and H.R. Guy. 2001. Structural models of the mscl gating mechanism. *Biophys. J.* 81:917–936.

Kale, L., R. Skeel, M. Bhandarkar, R. Brunner, A. Gursoy, N. Krawetz, J. Phillips, A. Shinozaki, K. Varadarajan, and K. Schulten. 1999. NAMD2: Greater scalability for parallel molecular dynamics. *J. Comput. Phys.* 151:283–312.

Fraczkiewicz, R., and W. Braun. 2002. Exact and efficient analytical calculation of the accessible surface areas and their gradients for macromolecules. *J. Comp. Chem.* 19:319–333.

Wesson, L., and D. Eisenberg. 1992. Atomic solvation parameters applied to molecular dynamics of proteins in solution. *Protein Sci.* 1:227–235.